Nucleation at twin boundaries in crystals undergoing phase transitions near singularities in phase diagrams. Direct observation of nuclei of low-symmetry phases in $NaNbO_3$

A. A. Bul'bich, V. P. Dmitriev, O. A. Zhelnova, and P. E. Pumpyan

Scientific-Research Institute of Physics at the State University, Rostov-on-Don
(Submitted 23 April 1990; resubmitted 28 April 1990)
Zh. Eksp. Teor. Fiz. **98**, 1108–1119 (September 1990)

Wedge-shaped nuclei of the *Pmnm* phase and domain-split nuclei of the ferroelectric *R* 3*c* phase were observed against the background of the *Pbma* phase at twin boundaries in $NaNbO_3$. A region of existence of equilibrium nuclei of the phases which could not form in the bulk of a crystal was found near a multicritical point in the phase diagram of a crystal containing a twin boundary. Crystals undergoing a first-order transition had a phase diagram split into a region (adjoining the tricritical point) where the transition involved formation and growth of equilibrium nuclei and another region where the transition involved motion of a nonequilibrium phase front.

There is still no reliable confirmation that in crystals undergoing a cascade or chain of structural phase transitions the appearance of nuclei of low-temperature phases is induced by twin boundaries created by high-temperature transitions. The presence of these nuclei influences macroscopic properties such as the strength, plasticity, internal friction, and susceptibility, as well as the thermodynamics of low-temperature transitions. Nucleation of a superconducting phase at twin boundaries has been observed already in Sn (Ref. 1), In (Ref. 2), Nb (Ref. 3), Re and Tl (Ref. 4), and in organic β-$(ET)_2X$ metals [here, $X = I_3$, IBr_2, or AuI_2, whereas ET is (ethylenedithio)tetrathiofulvalene].[5] This nucleation was deduced from the appearance of a magnetic moment in a sample and from a change in its resistance.[4]

Investigations of local structural phase transitions provide an opportunity for direct observation of nucleation of phases at inhomogeneities in a crystal. Such direct observations can be made by electron microscopy and by optical methods. In the former case a nucleus had been observed at a dislocation in the course of ordering of the alloy Ni_4Mo (Ref. 6) and during the α-Fe$\rightarrow\gamma$-Fe transformation,[7] and at the end of a fatigue crack in the course of a martensitic transformation,[8] whereas in the latter case it has been observed at a dislocation in NH_4Br (Ref. 9) and in iron garnets.[10] However the question of the possibility of formation as a result of a structural transition of a phase localized at a twin boundary has remained unresolved. The localized superconductivity has been described by the Ginzburg–Landau functional supplemented by a term containing a singularity,[4,11–16] which has made it possible to explain the phenomena associated with such superconductivity.[4] The singularity was attributed to a hypothetical enhancement of the electron–phonon interaction in a twin boundary plane (Ref. 11),[1)] and the phenomenon of nucleation at a twin boundary was assumed to occur only in the case of superconducting phase transitions.

It was shown in Refs. 18–20 that in the case of structural phase transitions we can expect the appearance of nuclei at twin boundaries, but the investigations were concerned with a second-order phase transition and a wide domain wall, which limited the analysis to a range of parameters close to the transition from the high-symmetry phase. In many crystals (including $NaNbO_3$ investigated by us) the process of nucleation occurs far from a transition from a high-symmetry phase and, therefore, a twin boundary is a thin layer. Moreover, the transitions are usually of the first order, but in some cases they can be described as close to a second-order transition. It would therefore be interesting to investigate nucleation of thin twin boundaries in the vicinity of a tricritical point in a phase diagram and also near multiphase points, where the multicomponent nature of the order parameter makes the structure and behavior of a nucleus qualitatively different from those predicted by models postulating one-component order parameters.

We shall report the first observation of nucleation at twin boundaries in the course of structural phase transitions. We shall show that nuclei of the *Pmnm* and *R* 3*c* phases appear at twin boundaries in the *Pbma* phase in $NaNbO_3$. We shall describe observations of nuclei with the phase boundary parallel to the twin boundary and of wedge-shaped nuclei of the *Pmnm* and *R* 3*c* phases, as well as splitting of the nuclei of the ferroelectric *R* 3*c* phase into subdomains.

We shall describe theoretically the nucleation of phases localized at a twin boundary in the vicinity of multiphase and tricritical points of the phase diagram. We shall show that in the vicinity of a multiphase point there is a region of existence of localized phases which cannot appear in the bulk of a crystal. We shall demonstrate that a crystal undergoing a first-order phase transition with properties close to a second-order transition exhibits a limited range of existence of equilibrium nuclei: this range becomes narrower and disappears away from the tricritical point. Therefore, a phase transition involving growth of equilibrium nuclei changes, on increase in the degree of proximity of a phase transition to one of the first order, and is replaced by a regime in which a transition involves motion of a nonequilibrium phase front. The same result is obtained for order–disorder transitions in the vicinity of the tricritical point in the phase diagram using the example describing the *Pbma*$\rightarrow$*Pmnm* phase transition in $NaNbO_3$. A description is given of the distribution of the order parameter in straight and wedge-shaped nuclei and of the structure of the boundary between subdomains in a nucleus.

1. NUCLEATION IN $NaNbO_3$ AT TWIN BOUNDARIES

Sodium niobate ($NaNbO_3$) undergoes a series of antiferrodistortion phase transitions in different temperature intervals:.

 0038-5646/90/090619-07$03.00

$$Pm3m \xrightarrow{913\ \text{K}} P4/mbm \xrightarrow{848\ \text{K}} Ccmm \xrightarrow{793\ \text{K}} Pnmm$$

$$\xrightarrow{753\ \text{K}} Pmnm \xrightarrow{643\ \text{K}} Pbma \xrightleftarrows{170\ \text{K}} R3c.$$

Moreover, the $R\,3c$ and $P\,2_1\,ma$ phases may be induced by an external critical field.[20,21] Following high-temperature transitions in the *Pbma* phase a crystal usually contains {100}, {110}, {1*k* 1} twin boundaries, which are described using the coordinates of a pseudocubic cell.[22] We shall consider $Pbma(P) \rightarrow Pmnm(R)$ and $Pbma \rightarrow R\,3c(N)$ phase transitions in the vicinity of a twin boundary.

We investigated $NaNbO_3$ crystals grown by the method of bulk spontaneous polarization from solutions in high-temperature Na_2O–Nb_2O_5–B_2O_3, Na_2O–Nb_2O_5–NaF–V_2O_5 melts. The use of polarization-optical (orthoscopic and conoscopic) methods in studies of phase transitions enabled us to identify the phases in accordance with the published data of structural investigations and to observe twins as well as twin boundaries, i.e., we were able to investigate a local region in a crystal.

A uniform temperature distribution throughout the investigated sample was ensured by incorporating a bulk cylindrical metal insert in a heating stage, but this did not prevent a weak temperature gradient, which was not determined. The rate of change of temperature was ~5 K/min. Fragments of the $P \rightarrow R$ phase transitions in a twinned $NaNbO_3$ crystal are shown in Fig. 1. The high contrast of domains of the *Pbma* phase, exhibiting symmetric extinction, was ensured using a $\lambda/4$ plate. All three orientations of the crystal structure of $NaNbO_3$ exhibited parallel extinction in the *Pmnm* phase, so that in $45° \pm \pi/2$ position at least the orientational states corresponding to a birefringence ~0.2–0.22 had a bright interference coloring and differed sharply from the original *Pbma* phase. During the initial moments of the phase transition a nucleus of the *Pmnm* phase appeared at a twin boundary in the original phase and this nucleus was wedge-shaped. A nucleus at the edge of a plate appeared almost simultaneously (Fig. 1a).

An increase in the volume of the new phase was due to "growth" of the wedge-shaped nucleus along a {100} twin boundary of the original phase and due to sideways motion of a phase front from the edge of the plate (Fig. 1b). A cinematographic study of the transition process demonstrated that it consisted of a series of successive jumps of the phase front. In other words, finite nuclei (Fig. 1a) appeared in a sample when it reached a certain temperature at a twin boundary and its edge. A further change in the temperature of the crystal showed that in a range amounting to about a hundred kelvin there was no growth of nuclei and then the size of a nucleus changed abruptly (Figs. 1b and 1c) in a time less than 1/30th of a second.

The jump-like motion of a phase front occurred also in a gradient-free temperature field when a heating element evaporated on the surface of glass, parallel to the surface of the crystal plate, was used. In the case of the $Pbma \rightarrow R\,3c$ transition which occurred as a result of cooling the twin boundaries of the original phase at the edge of the plate were again preferential positions for the appearance of nuclei of the new phase. Figure 2a shows an $NaNbO_3$ crystal revealing clearly interference fringes in the region of an overlap of the components of 60° twins of the *Pbma* phase with {110} boundaries and different nature of extinction, whereas Fig. 2b shows the polysynthetically twinned phase $R\,3c$ in the region of twin boundaries of the original phase. The appearance of nuclei of the $R\,3c$ phase in an $NaNbO_3$ crystal exhibiting a parallel extinction of the components of a 60° twin in the original *Pbma* phase with a {110} boundary is demonstrated in Fig. 2c. The $Pbma \rightarrow R\,3c$ phase boundary was parallel to the (100) and (110) planes of the pseudocubic cell or it was wedge-shaped. The $Pbma \rightarrow R\,3c$ transition in single-domain $NaNbO_3$ plates in which parallel extinction occurred in the original phase exhibited growth of polysynthetically twinned wedges from the edge of the plate. Therefore, the phase transition was due to motion of plane boundaries and growth of wedges. The $P \rightarrow N$ transition, like the $P \rightarrow R$ one, usually occurred as a result of motion of phase boundaries in the form of a series of consecutive jumps.

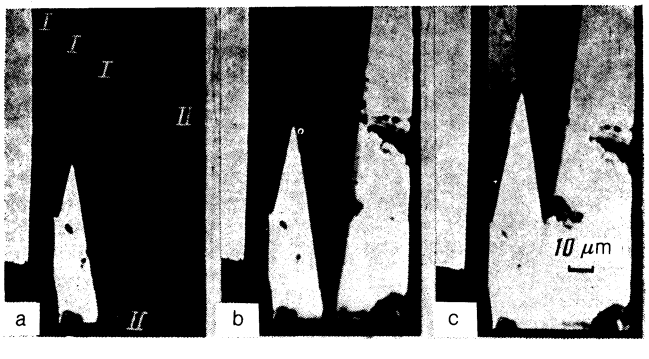

FIG. 1. Fragments illustrating the $Pbma \rightarrow Pmnm$ phase transition in an $NaNbO_3$ crystal containing 19° twins in the *Pbma* phase with boundaries of the {100} type in coordinates of the pseudocubic cell (magnification by a factor of 600): a) wedge-shaped nucleus of the *Pmnm* phase in the region of the {100} twin boundary; I is the twin boundary and II is the edge of the crystal; b) "growth" of a wedge-shaped nucleus of the *Pmnm* phase through a crystal along the boundary and a considerable increase in the volume of the *Pmnm* phase due to the motion of the phase front from the edge of the plate; c) "merging" of two nuclei of the *Pmnm* phase.

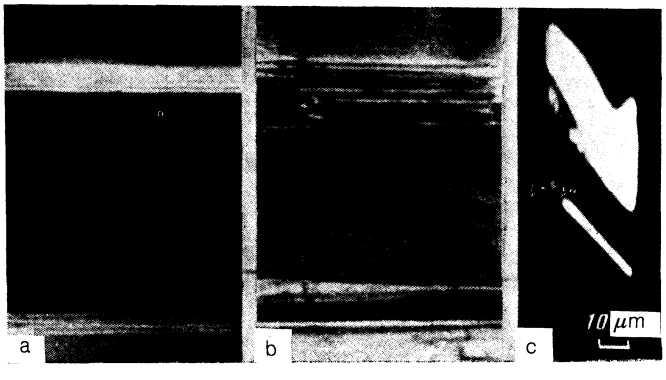

FIG. 2. Crystal of $NaNbO_3$ in the *Pbma* phase (a) and the initial moment of the $Pbma \rightarrow R\,3c$ phase transition (b); magnification by a factor of 600. The dark and bright bands in the region of the localized phase (b) represent splitting of a nucleus into subdomains with different directions of the polarization vector. The nucleus of the $R\,3c$ phase (c) (represented by the bright regions in the photograph) is shown in the region of twin boundaries of the {110} type of the original *Pbma* phase (the main part of the crystal is dark).

2. LOCAL PHASE TRANSITION AT A TWIN BOUNDARY IN THE VICINITY OF A MULTIPHASE POINT

We shall consider a low-temperature phase transition described by a two-component order parameter (η_1,η_2) occurring in the "field" of an order parameter corresponding to a high-temperature phase transition. If the difference between the temperatures of these two transitions is large, a twin boundary generated by the high-temperature transition is thin and makes a contribution[20] given by $\sim\cosh^{-2}(z/z_0)$ (z_0 is the twin boundary thickness such that $z_0\to 0$), which can be approximated satisfactorily by the δ function:

$$F=\int_{-\infty}^{+\infty}\left\{\frac{g}{2}(\dot\eta_1^2+\dot\eta_2^2)+\frac{\alpha_1}{2}(\eta_1^2+\eta_2^2)+\frac{\alpha_2}{4}(\eta_1^2+\eta_2^2)^2+\frac{\gamma}{2}\eta_1^2\eta_2^2-A\delta(z)(\eta_1^2+\eta_2^2)\right\}S\,dz, \tag{1}$$

where $\eta\equiv\partial\eta/\partial z$ and g, α_i, γ are phenomenological parameters. On substitution of $A=0$ we find that the potential of Eq. (1) describes three homogeneous phases:

I. $\eta_1=\eta_2=0$ $(\alpha_1>0)$;

in the space of $\mathbf{E}_2$ of the order parameter components the symmetry group of this phase is $L=C_{4v}$;

II. $\eta_1\neq 0$, $\eta_2=0$ $(\alpha_1<0,\ \gamma>0)$, $L=C_s$;

III. $\eta_1=\eta_2\neq 0$ $(\alpha_1<0,\ \gamma<0)$ $L=C_s$ (Fig. 3).

The transition from the homogeneous phase $\eta_1=\eta_2=0$ to a localized phase with the symmetry C_s occurs at a branching point α_1^* of the following system of equations:

$$\begin{cases}g\ddot\eta_1=\alpha_1\eta_1+\alpha_2\eta_1(\eta_1^2+\eta_2^2)+\gamma\eta_1\eta_2^2-2A\delta(z)\eta_1,\\ g\ddot\eta_2=\alpha_1\eta_2+\alpha_2\eta_2(\eta_1^2+\eta_2^2)+\gamma\eta_1^2\eta_2-2A\delta(z)\eta_2,\end{cases} \tag{2}$$

$$\alpha_1^*=\alpha_0=A^2/g.$$

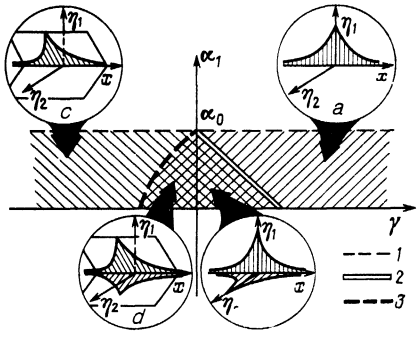

FIG. 3. Phase diagram of local phase transitions and of transitions in the bulk of a crystal described by the potential of Eq. (1): $\alpha_1>0$ is the range of existence of phase I; $\alpha_1<0$, $\gamma>0$ is the phase II; $\alpha_1<0$, $\gamma<0$ is the phase III. 1) Branching line $\alpha=\alpha_0$; 2) line $k=\alpha_2^{-1}$; 3) line $k=-2(\alpha_2+\gamma)^{-1}$ [see Eq. (5′)]. The shaded region represents the existence of a local phase with the symmetry C_s. The double shading is the range of existence of a localized phase with the symmetry C_1. The insets show the distributions of the order parameter in a nucleus with the symmetry C_s (a, c) and C_1 (b, d). The regions of formation of the nuclei in the phase diagram are identified by arrows.

The principal term of the branched-off solution is

$$\eta_1=\xi_1\psi_0(z),\quad \eta_2=\xi_2\psi_0(z),$$

where

$$\psi_0(z)=\exp(-A|z|/g).$$

Substitution of this solution into the functional of Eq. (1) gives a potential describing nucleation at a twin boundary outside the direct vicinity of a multiphase point:

$$F(\xi_1,\xi_2)=\frac{Sg}{A}\{{}^1\!/_2(\alpha_1-\alpha_0)(\xi_1^2+\xi_2^2)+{}^1\!/_8\alpha_2(\xi_1^2+\xi_2^2)^2+{}^1\!/_4\gamma\xi_1^2\xi_2^2\}. \tag{3}$$

The phase diagram of the potential described by Eq. (3) repeats the phase diagram of the potential (1) representing homogeneous bulk phases, apart from a shift by α_0 (Fig. 3). The right-hand side of the phase diagram characterized by $0<\alpha_1<\alpha_0$, $\gamma>0$ represents the appearance of a localized phase

$$\xi_2=0,\quad \xi_1=[2(\alpha_0-\alpha_1)/\alpha_2]^{1/2},$$

whereas as on the left-hand side in the range $0<\alpha_1<\alpha_0$, $\gamma<0$, we have the phase

$$\xi_1=\xi_2=[2(\alpha_0-\alpha_1)/(2\alpha_2+\gamma)]^{1/2}.$$

The two localized phases characterized by $\xi\neq 0$, $\xi_2=0$ and $\xi_1=\xi_2\neq 0$ have the C_s symmetry in the $\mathbf{E}_2$ space. However, in the vicinity of a certain point $(\alpha=\alpha_0,\gamma=0)$ in the phase diagram there is a range where the localized phase with the C_1 symmetry can exist: $\eta_1(z)\neq\eta_2(z)\neq 0$. We shall consider branching off of the solutions with the C_1 symmetry from the solution with the C_s symmetry corresponding to a localized phase characterized by $\xi_1\neq 0$, $\xi_2=0$:

$$\eta_1=\xi_1\exp(-A|z|/g)+v(z),$$

$$\eta_2=\eta_2(z),\quad v(\pm\infty)=\eta_2(\pm\infty)=0.$$

The branching occurs when the linear term in Eq. (2) for η_2 vanishes:

$$g\ddot\eta_2=\{\alpha_1+2(\alpha_0-\alpha_1)(1+\gamma/\alpha_2)\exp(-2A|z|/g)-2A\delta(z)\}\eta_2. \tag{4}$$

The principal term of the branched-off solution is

$$\eta_2=\zeta I_\nu(b\exp(-A|z|/g)),\quad v\sim\zeta^2,$$

$$\nu^2=\frac{\alpha_1}{\alpha_0},\quad b^2=2(1-\nu^2)\left(1+\frac{\gamma}{\alpha_2}\right), \tag{5}$$

where ζ is the amplitude and I_ν is a modified Bessel function. The boundary condition $bI_\nu'(b)=I_\nu(b)$, which follows from the singular term of Eq. (4) (Ref. 24), is an equation for a branching line in the phase diagram. In the vicinity of the point $\alpha_1=\alpha_0$, $\gamma=0$ we have $b\ll 1$ and this equation then becomes

$$\alpha_1=\alpha_0-4\alpha_0k\gamma, \tag{5′}$$

where $k=\alpha_2^{-1}$ if $\gamma>0$. If $\gamma<0$, the branching originates from the solution

$\xi_1=\xi_2\neq 0, \quad k=-2(\alpha_2+\gamma)^{-1}$.

Therefore, in the vicinity of the tricritical point $\alpha_1=\alpha_0, \gamma=0$ of the phase diagram there is a region where a two-parameter localized phase may be realized and this phase does not have a bulk analog (represented by the region of double shading in Fig. 3). A localized phase which cannot form in the bulk of a crystal has been observed also in the vicinity of a dislocation in an iron garnet.[25]

3. APPEARANCE OF NUCLEI AT TWIN BOUNDARIES DUE TO TRANSITIONS BETWEEN LOW-SYMMETRY PHASES

We shall now consider nucleation in the case of an order–order transition between low-symmetry phases by taking as an example a transition described by two different order parameters η and φ:

$$F=\int_V \{g_1\dot\eta^2+a_1\eta^2+a_2\eta^4+g_2\dot\varphi^2+b_1\varphi^2+b_2\varphi^4+c\eta^2\varphi^2 +A\delta(x)\eta^2-B\delta(x)\varphi^2\}S\,dx. \tag{6}$$

A group-theoretic analysis (Sec. 5) shows that the potential (6) can be used to describe nucleation in the course of the $P\leftrightarrow R$ phase transition in $NaNbO_3$. The quantities A and B in Eq. (6) determine the strength of the interaction of the order parameter with a twin boundary. If $A=B=0$, we have $4a_2b_2-c^2<0$ and the potential of Eq. (6) describes three homogeneous phases:[26] $\eta=\varphi=0$; $P(\eta\neq 0, \varphi=0)$; $R(\eta=0, \varphi\neq 0)$ (see Fig. 4).

The system of equations

$$\begin{cases} g_1\ddot\eta=a_1\eta+2a_2\eta^3+c\eta\varphi^2+2A\delta(x)\eta, \\ g_2\ddot\varphi=b_1\varphi+2b_2\varphi^3+c\eta^2\varphi-2B\delta(x)\varphi, \end{cases} \tag{7}$$

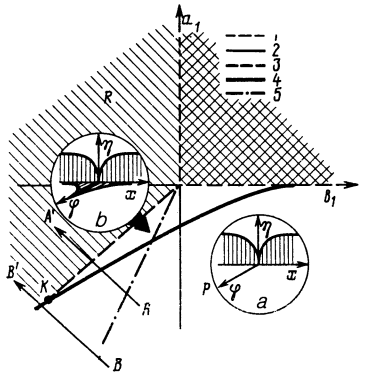

FIG. 4. Phase diagram in the vicinity of the triple point ($a_1=b_1=0$) of the potential (6) in the case when $4a_2b_2-c^2<0$, $c>0$. The phases with $\eta=\varphi=0$ (double shading), R (single shading), and P coexist in the diagram. 1) Lines of second-order transitions from the $\eta=\varphi=0$ phase to the phases P and R; 2) coordinate axes; 3) line $a_1=b_1(a_2/v_2)^{1/2}$ of the first-order transition $P\leftrightarrow R$; lines 4 and 5 represent Eqs. (11) and (13), respectively. The insets show a quasihomogeneous distribution of the order parameter of Eq. (8) in the P phase in the vicinity of the twin boundary (a) and the distribution of the order parameters η and φ [Eqs. (8) and (9)] corresponding to the appearance of a nucleus of the phase R against the background of the phase P (b). The range of existence of the nucleus is identified by an arrow in the phase diagram. The thermodynamic paths A–A' and B–B' represent the situations in which the appearance of equilibrium nuclei is possible and impossible, respectively.

follows from Eq. (6) and has the exact solution for the P phase:

$$\eta=\left(\frac{|a_1|}{2a_2}\right)^{1/2}\operatorname{th} t, \quad \varphi(x)=0, \tag{8}$$

where

$$t=(|a_1|/2g_1)^{1/2}|x|+p; \quad \operatorname{th} p=[(D^2+2)^{1/2}-D]/\sqrt{2},$$

$$D=A(|a_1|g_1)^{-1/2}.$$

The solution given by Eq. (8) is shown in Fig. 4a.

The appearance of a localized phase $\varphi(x)\neq 0$ [$\varphi(\pm\infty)=0$] occurs at a branching point of the system (7). The branched-off solution is

$$\varphi=\xi\operatorname{ch}^{-\varepsilon}tF\left(\varepsilon-s,\ \varepsilon+s+1,\ \varepsilon+1,\ \frac{1-\operatorname{th} t}{2}\right), \tag{9}$$

where

$$\varepsilon=\left\{\frac{[2b_1/|a_1|+c/2a_2]g_1}{g_2}\right\}^{1/2}, \quad 2s=\left\{\frac{1+4cg_1}{a_2g_2}\right\}^{1/2}-1,$$

F is the hypergeometric function, and ξ is the amplitude. The equation for the branching line is given implicitly by the boundary condition at $t=p$:

$$2\left\{\varepsilon\operatorname{th} p-\frac{2B}{g_2}\left(\frac{g_1}{2|a_1|}\right)^{1/2}\right\} =\operatorname{ch}^{-2}p\frac{\partial}{\partial z}\ln F(\varepsilon-s, \varepsilon+s+1, \varepsilon+1, z), \tag{10}$$

where $(1-\tanh p)/2$. If $A\ll 1$, the equation for the branching line becomes $a_1=-2a_2B^2c^{-1}g_2^{-1}+2a_2b_1c^{-1}$ (line 4 in Fig. 4). The point K of intersection of this line with the line representing the first-order transitions between the bulk phases $P\leftrightarrow R$

$$a_1=b_1(a_2/b_2)^{1/2}$$

(line 3 in Fig, 4) has the coordinates

$$a_1^{(k)}=-2a_2B^2/Q, \quad b_1^{(k)}=-2(a_2b_2)^{1/2}B^2/Q,$$

where

$$Q=cg_2\{1-2(a_2b_2)^{1/2}/c\}.$$

This intersection means that to the left of the point K the existence of equilibrium nuclei is inconvenient, so that in the thermodynamic path A–A' (Fig. 4) a phase transition results from nucleation and growth of equilibrium nuclei localized at a twin boundary, whereas in the B–B' path this occurs as a result of motion of a nonequilibrium front. In the opposite limiting case when $A\gg 1$ and $B\ll 1$, the branching occurs along the line

$$a_1=\frac{4g_1b_1g_2^{-1}}{\{(1+4g_1cg_2^{-1}a_2^{-1})^{1/2}-1\}}.$$

This is line 5 in Fig. 4 and it lies below line 3 if $c<4g_1b_2g_2^{-1}$, or $4a_2b_2-c^2>8g_1b_2(2b_2-c)g_2^{-1}$ when $c>4g_1b_2g_2^{-1}$. In this case the phase transition involves the formation and growth of nuclei at a twin boundary. However, if these inequalities are not satisfied, then equilibrium nuclei do not

appear and a phase transition may involve motion of a front.

It should be pointed out that the symmetry of a unit cell of a nucleus (Fig. 4b) is exactly the same as the symmetry of the growing phase $\eta \neq \varphi \neq 0$. Therefore, a nucleus of a phase which cannot appear in the bulk of a crystal forms at a twin boundary.

4. PHASE DIAGRAM OF A LOCAL TRANSITION IN THE VICINITY OF A TRICRITICAL POINT

A phase transition occurring on a twin boundary in the vicinity of a tricritical point $\alpha = \beta = 0$ is described well by the following potential:

$$F = \int_V \{ {}^1/_2 g\dot{\eta}^2 + {}^1/_2\alpha\eta^2 + {}^1/_4\beta\eta^4 + {}^1/_6\gamma\eta^6 - A\delta(z)\eta^2 \} S\, dz. \tag{11}$$

If $\beta > 0$, the local phase transition is of the second order with a branching point $\alpha = \alpha_0$.

The equation of state which follows from Eq. (11) can be solved exactly if it is assumed that $\beta < 0$, which gives

$$\eta = \frac{2(3\alpha)^{1/2}}{\left\{ |\Delta|^{1/2} \operatorname{sh}\left(2\left(\frac{\alpha}{g}\right)^{1/2} |z| + p \right) + 3|\beta| \right\}^{1/2}}, \tag{12}$$

where

$$p = \ln\{([9\beta^2 D^2 - \Delta(D^2-1)]^{1/2} - 3|\beta|D)(D-1)^{-1}|\Delta|^{-1/2}\},$$
$$\Delta = 9\beta^2 - 48\alpha\gamma, \quad D = A(\alpha g)^{-1/2}.$$

The solution (12) is valid in the range $3\beta^2/16\gamma < \alpha < A^2/g + 3\beta^2/16\gamma$. Substitution of Eq. (12) into the functional (11) gives the equilibrium free energy E_0 of a nucleus at a twin boundary (see the Appendix). A numerical analysis of this expression shows that in the range of values $\beta/\gamma \in [0, -5]$ the expression for line 3 in Fig. 5 can be approximated by

$$\alpha = \alpha_0 + 3\beta^2\varkappa/16\gamma,$$

where $\varkappa \approx 0.75$ if $\beta/\gamma \in [0, -2{,}2]$ and $\varkappa \approx 0.82$ if $\beta/\gamma \in [-4, -5{,}5]$. Then, the point T of intersection of lines 3 and 4 (Fig. 5) has the coordinates $\beta_T \approx 5{,}5(\alpha_0\gamma)^{1/2}$ and $\alpha_T \approx 5{,}7\alpha_0$.

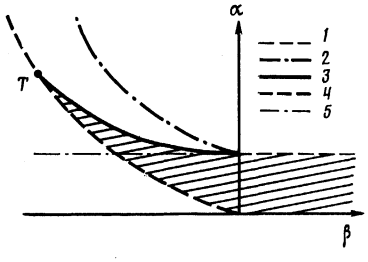

FIG. 5. Phase diagram of a local transition on a twin boundary in the vicinity of the tricritical point $\alpha = \beta = 0$: 1) line of a local second-order phase transition characterized by $\alpha = \alpha_0$ and $\beta > 0$; 2) line of the absolute loss of stability by the localized phase: $\alpha = \alpha_0 + 3\beta^2/16\gamma$; 3) line of equality of the energies of a twin boundary with and without a nucleus: $\alpha = \alpha_0 + 3\beta^2\varkappa/16\gamma$; 4) first-order transition in the bulk of a crystal: $\alpha = 3\beta^2/16\gamma$; 5) line $\alpha = \alpha_0$ for $\beta < 0$ (the $\eta = 0$ phase is unstable below this line).

When line 3 of the phase diagram (Fig. 5) is reached, a nucleus of a finite size appears at a twin boundary. Further cooling causes its growth so that it fills the whole crystal when line 4 is reached. However, if the thermodynamic path passes to the left of the point T, the appearance of nuclei is thermodynamically favorable. In this case crossing of line 4 in the phase diagram of a crystal with a twin boundary or in the case of a transition from the edge of a crystal the phase front collapses and the whole crystal assumes the $\eta \neq 0$ phase.

5. DISCUSSION

In this section we shall show nucleation at a twin boundary in an $NaNbO_3$ crystal (Sec. 1) can be described using the potential of Eq. (6) (Sec. 3) and we shall propose an explanation for the wedge shape of a nucleus and for a transition layer between subdomains in nuclei observed due to $P \to N$ transitions in $NaNbO_3$.

Without going into the fairly conventional procedure of determination of the orders parameters and their components, differing from zero for the phases P and R of interest to us, we shall give the final result of a group-theoretic analysis. The transition of each of the P and R phases is related to two order parameters, one of which (common to P and R) transforms in accordance with the three-dimensional irreducible representation $\tau_1(k_{11})$ of the space group O_h^1 symmetry of the original cubic phase. Moreover, in the case of both phases only one out of three components of the order parameter differs from zero, i.e., a transition may occur in the "field" of this component of the order parameter with a change in the other two components. The latter have the symmetry of a single direction in the reciprocal space $k_8 = \mu b_3$ and for one of them we have $\mu_1 = 1/4$ (P phase) and for the other $\mu_2 = 1/6$ (R phase). Bearing in mind the special features of the distortion of the structure on transition to the phase P, we can show that both these components of the order parameter transform in accordance with the $\tau_5(k_8)$ representation. For completeness, we should point out that formation of the rhombohedral polar N phase with the $C_{3v}^6(R\,3c)$ symmetry is related to two three-component order parameters, the first of which is the same $\tau_5(k_{11})$ as in the case of the transitions to the P and R phases, but in this case all the components differ from zero and are equal. The second order parameter is the spontaneous polarization such that $P_x = P_y = P_z$. Next, direct calculations can show that the nonequilibrium thermodynamic potential of the $P \to R$ transition contains only invariances of the second and fourth power in respect of the order parameter $\tau_5(k_8)$, corresponding to these phases, and a mixed biquadratic invariant, i.e., the $P \to R$ transition is described by the potential (6).

We shall show that in the field of a temperature gradient $\alpha = \tilde{\alpha} + \omega x$ a nucleus localized at a twin boundary lying in the $y = 0$ plane is wedge-shaped. We shall assume that the surrounding crystal occupies a region $x \geqslant 0$ and also that $(\partial\eta/\partial x)|_{x=0} = 0$, where $\tilde{\alpha}$ is the value of α at the $x = 0$ edge of the crystal. The linear part of the equation of state becomes

$$g\left(\frac{\partial^2\eta}{\partial x^2} + \frac{\partial^2\eta}{\partial y^2} \right) = (\tilde{\alpha} + \omega x - 2A\delta(y))\eta. \tag{13}$$

Equation (13) gives the value $\tilde{\alpha}_0 = A^2/g - 1.02(\omega^2 g)^{1/3}$ for the branching point and the branched-off solution is

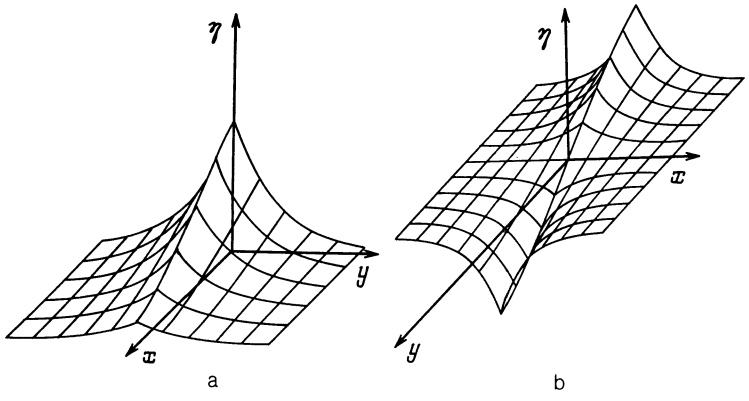

FIG. 6. a) Distribution of the order parameter of Eq. (14) in the vicinity of a twin boundary, emerging on the edge of a crystal in the field of a temperature gradient. A crystal is located in the region $x \geqslant 0$ and a twin boundary is in the $y = 0$ plane. b) Distribution of the order parameter in the vicinity of a circulation line. A twin boundary is located in the $x = 0$ plane.

$$\eta = \xi \exp\left\{-\frac{A}{g}|y|\right\} \mathrm{Ai}\left\{\left(\frac{a}{g}\right)^{1/3} x - 1{,}02\right\}, \qquad (14)$$

where $\mathrm{Ai}(x)$ is the Airy function and ξ is the amplitude. The distribution of the order parameter of Eq. (14) is shown in Fig. 6a. The line corresponding to the level $\eta(x, y) = \text{const}$ is in the form of a wedge similar to the wedge-shaped nuclei of the R phase in Fig. 1.

A transition from the antiferroelectric phase P to the ferroelectric phase N ($R\,3c = C_{3v}^6$) in $NaNbO_3$ causes splitting of the nucleus of the N phase localized at a twin boundary into a system of domains shown in Fig. 2b. The boundary between these domains is a one-dimensional defect of the order parameter field, i.e., it is a circulation line.[19]

Near the branching point this boundary changes into a transition layer between the subdomains of the nucleus and the thickness of this layer diverges in the limit $T \to T_0$, which is the branching temperature. The distribution of the order parameter in the vicinity of such a layer is an extremum of the functional

$$F(\eta) = \int_V \left\{\frac{g}{2}\left[\left(\frac{\partial \eta}{\partial x}\right)^2 + \left(\frac{\partial \eta}{\partial y}\right)^2\right] + \frac{\alpha}{2}\eta^2 + \frac{\beta}{4}\eta^4 - A\delta(x)\eta^2\right\} L\,dx\,dy, \qquad (15)$$

where L is the length of the crystal along the z axis. In the vicinity of the branching point α_0 we can find the solution of the equation of state in the form $\eta = \xi(y)\psi_0(x)$. We shall then obtain the following functional for $\xi(y)$:

$$F(\xi) = \frac{Lg}{A}\int \left\{ {}^1/_2 g\left(\frac{\partial \xi}{\partial y}\right)^2 + {}^1/_2(\alpha - \alpha_0)\xi^2 + {}^1/_8\beta\xi^4\right\} dy. \qquad (16)$$

The equation for $\xi(y)$ which follows from the condition for the minimum of the functional (16) has the solution

$$\xi(y) = [2(\alpha_0 - \alpha)/\beta]^{1/2} \mathrm{th}\{[(\alpha_0 - \alpha)/2g]^{1/2} y\}$$

with the transition layer thickness $l\alpha(\alpha_0 - \alpha)^{-1/2}$ diverging at the branching point. The distribution of the order parameter in the transition layer is shown in Fig. 6b.

6. CONCLUSIONS

The appearance of a localized phase, which does not form in the bulk of a crystal, is a common occurrence. Such a phase may be induced by a defect creating an homogeneity and by the edge of a crystal. It can appear because an inhomogeneous distribution of the order parameter of the original phase alters the conditions for the loss of stability by precipitation of a condensate with the second order parameter, compared with the conditions of the loss of stability of homogeneous phases. The precipitated phase with the second-order parameter is localized in the region of an increase or a fall of the first order parameter, depending on the sign of the interaction constant. This is most likely to occur near a multiphase point, because the anisotropy of a crystal in the space of the components of the order parameter **E** is weak in this region. On the other hand, the conclusion about the limited range of existence of nuclei (point T) in the case of a first-order phase transition, which is the result of the exact solution of Eq. (12), applies only to inhomogeneities with a small radius of the falling region. The coordinates of the point T are governed by the temperature interval α_0 of the existence of nuclei. In our experiments, and also in Refs. 4 and 10, this interval was $\alpha_0 \sim -0.1$–5 K. The point T was then in the range of validity of the Landau theory. However, no rigorous theoretical results for long-range inhomogeneities and the experimental results demonstrate that in the case of a crack creating an inhomogeneity proportional to $r^{-1/2}$ a nucleus appears even in the case of such a definite first-order transition as that from the tetragonal to the monoclinic phase of ZrO_2 (Ref. 27).

The authors are grateful to A. L. Korzhenevskiĭ and A. K. Tagantsev for discussing the results, and to M. L. Kraĭzman who provided us with his program producing three-dimensional images.

APPENDIX

The expression for the equilibrium free energy of a nucleus in the case of a first-order phase transition is

$$F_0 = G_1\left\{1 - \frac{\Delta^{1/2}\,\mathrm{ch}\,p}{\Delta^{1/2}\,\mathrm{sh}\,p + 3|\beta|} - \frac{3|\beta|}{(48\alpha\gamma)^{1/2}}Y\right\} + G_2\left\{\frac{3|\beta|}{48\alpha\gamma}\left(1 - \frac{\Delta^{1/2}\,\mathrm{ch}\,p}{\Delta^{1/2}\,\mathrm{sh}\,p + 3|\beta|}\right) - \frac{1}{3}\frac{\Delta^{1/2}\,\mathrm{ch}\,p}{(\Delta^{1/2}\,\mathrm{sh}\,p + 3|\beta|)^2} - \frac{9\beta^2 - 16\alpha\gamma}{(48\alpha\gamma)^{3/2}}Y\right\},$$

where

$$G_1=\frac{3}{4}\frac{|\beta|}{\gamma}(\alpha g)^{1/2},\quad G_2=18(\alpha^3 g)^{1/4},$$

$$\Delta=48\alpha\gamma-9\beta^2,\quad D=A(\alpha g)^{-1/2},$$

$$p=\ln\left\{\frac{(-3|\beta|D+[9\beta^2D^2+\Delta(D^2-1)]^{1/2})}{(D-1)\Delta^{1/2}}\right\},$$

$$Y=\ln\frac{(48\alpha\gamma)^{1/2}+3|\beta|-\Delta^{1/2}}{(48\alpha\gamma)^{1/2}-3|\beta|+\Delta^{1/2}}$$

$$-\ln\frac{(48\alpha\gamma)^{1/2}+3|\beta|\,\mathrm{th}(p/2)-\Delta^{1/2}}{(48\alpha\gamma)^{1/2}-3|\beta|\,\mathrm{th}(p/2)+\Delta^{1/2}}.$$

[1)]It follows from the recently published results[17] that the appearance of a localized superconductivity at a twin boundary in tin at temperatures $T_0>T_c$ is related to its defect structure, whereas in the case of defect-free twin boundaries we have $T_0<T_c$ and, therefore, the electron–phonon interaction is weaker at a twin boundary.

[1]M. S. Khaĭkin and I. N. Khlyustikov, Pis'ma Zh. Eksp. Teor. Fiz. **33**, 167 (1981) [JETP Lett. **33**, 158 (1981)].
[2]I. N. Khlyustikov and M. S. Khaĭkin, Pis'ma Zh. Eksp. Teor. Fiz. **34**, 207 (1981) [JETP Lett. **34**, 198 (1981)].
[3]I. N. Khlyustikov and S. I. Moskvin, Zh. Eksp. Teor. Fiz. **89**, 1846 (1985) [Sov. Phys. JETP **62**, 1065 (1985)].
[4]I. N. Khlyustikov and A. I. Buzdin, Usp. Fiz. Nauk **155**, 47 (1988) [Sov. Phys. Usp. **31**, 409 (1988)].
[5]A. V. Zvarykina, M. V. Kartsovnik, V. N. Laukhin *et al.*, Zh. Eksp. Teor. Fiz. **94**(9), 277 (1988) [Sov. Phys. JETP **67**, 1891 (1988)].
[6]S. N. Zolotarev, I. B. Sidorova, Yu. A. Skakov, and V. A. Solov'ev, Fiz. Tverd. Tela (Leningrad) **20**, 775 (1978) [Sov. Phys. Solid State 20, 450 (1978)].
[7]Nguyen Hoang Ngi, A. I. Novikov, Yu. A. Skakov, and V. A. Solov'ev, Fiz. Met. Metalloved. **64**, 915 (1987).
[8]E. Hornbogen, Acta Metall. **28**, 147 (1987).
[9]M. V. Belousov and B. E. Vol'f, Pis'ma Zh. Eksp. Teor. Fiz. **31**, 348 (1980) [JETP Lett. **31**, 317 (1980)].
[10]V. K. Vlasko-Vlasov and M. V. Indenbom, Zh. Eksp. Teor. Fiz. **86**, 1084 (1984) [Sov. Phys. JETP **59**, 633 (1984)].
[11]V. V. Averin, A. I. Buzdin, and L. N. Bulaevskiĭ, Zh. Eksp. Teor. Fiz. **84**, 737 (1983) [Sov. Phys. JETP **57**, 426 (1983)].
[12]A. I. Buzdin, L. N. Bulaevskiĭ, and S. V. Panyukov, Zh. Eksp. Teor. Fiz. **87**, 299 (1984) [Sov. Phys. JETP **60**, 174 (1984)].
[13]A. I. Buzdin and N. A. Khvorikov, Zh. Eksp. Teor. Fiz. **89**, 1857 (1985) [Sov. Phys. JETP **62**, 1071 (1985)].
[14]A. F. Andreev, Pis'ma Zh. Eksp. Teor. Fiz. **46**, 463 (1987) [JETP Lett. **46**, 584 (1987)].
[15]A. A. Abrikosov and A. I. Buzdin, Pis'ma Zh. Eksp. Teor. Fiz. **47**, 204 (1988) [JETP Lett. **47**, 247 (1988)].
[16]A. V. Gurevich and R. G. Mints, Pis'ma Zh. Eksp. Teor. Fiz. **48**, 196 (1988) [JETP Lett. **48**, 213 (1988)].
[17]I. N. Khlyustikov, Zh. Eksp. Teor. Fiz. **96**, 2073 (1989) [Sov. Phys. JETP **69**, 1171 (1989)].
[18]E. G. Galkina, É. A. Zavadskiĭ, V. I. Kamenev *et al.*, Fiz. Tverd. Tela (Leningrad) **28**, 1723 (1986) [Sov. Phys. Solid State **28**, 954 (1986)].
[19]É. B. Sonin and A. K. Tagantsev, Zh. Eksp. Teor. Fiz. **94**(2), 315 (1988) [Sov. Phys. JETP **67**, 396 (1988)].
[20]A. A. Bul'bich and Yu. M. Gufan, Zh. Eksp. Teor. Fiz. **94**(6), 121 (1988) [Sov. Phys. JETP **67**, 1153 (1988)].
[21]C. N. W. Darlington, J. Appl. Phys. **43**, 4951 (1972).
[22]O. A. Zhelnova, O. E. Fesenko, and V. G. Smotrakov, Fiz. Tverd. Tela (Leningrad) **28**, 267 (1986) [Sov. Phys. Solid State **28**, 144 (1986)].
[23]O. A. Zhelnova and O. E. Fesenko, Ferroelectrics **75**, 469 (1987).
[24]A. V. Gurevich and R. G. Mints, Usp. Fiz. Nauk **142**, 61 (1984) [Sov. Phys. Usp. **27**, 19 (1984)].
[25]V. K. Vlasko-Vlasov, L. M. Dedukh, and V. I. Nikitenko, Fiz. Tverd. Tela (Leningrad) **23**, 1857 (1981) [Sov. Phys. Solid State **23**, 1085 (1981)].
[26]Yu. M. Gufan, *Structural Phase Transitions* [in Russian], Nauka, Moscow (1982).
[27]L. K. Lenz and A. H. Heuer, J. Am. Ceram. Soc. **65**, 192 (1982).

Translated by A. Tybulewicz